106992

ENTERED

ELSEVIER

Journal of Contaminant Hydrology 53 (2001) 41–61

JOURNAL OF Contaminant Hydrology

www.elsevier.com/locate/jconhyd

Analytical solutions of contaminant transport from finite one-, two-, and three-dimensional sources in a finite-thickness aquifer

Eungyu Park *, Hongbin Zhan

Department of Geology and Geophysics, Texas A&M University, College Station, TX 77843-3115, USA

Received 26 September 2000; received in revised form 27 April 2001; accepted 1 May 2001

Abstract

Analytical study of contaminant transport from a finite source in a finite-thickness aquifer is most useful in hydrological and environmental sciences and engineering but rarely investigated in previous studies. This paper provides analytical solutions of contaminant transport from one-, two-, and three-dimensional finite sources in a finite-thickness aquifer using Green's function method. A library of unpublished analytical solutions with different finite source geometry is provided. A graphically integrated MATLAB® script is developed to calculate the temporal integrations in the analytical solutions and obtain the final solutions of concentration. The analytical solutions are examined by reproducing the solutions of some special cases discussed in previous studies. The sensitivities of the line source solutions to source geometry, dispersion coefficients, and distance to the source are tested. The contaminant concentration in the near field is found to be sensitive to the source geometry and anisotropy of the dispersion coefficients. The contaminant concentration in the far field is found to be much less sensitive to the source geometry. The physical insights of the analytical solutions are interpreted. © 2001 Elsevier Science B.V. All rights reserved.

Keywords: Analytical solution; Contaminant transport; Green's function; Advection–dispersion equation; Effect of geometry

1. Introduction

Contaminant transport in the subsurface has been one of the most important research topics in the hydrological sciences and engineering in the last four decades (Bear, 1972;

* Corresponding author. Tel.: +1-979-845-9683; fax: +1-979-845-6162.
E-mail address: park@hydrog.tamu.edu (E. Park).

0169-7722/01/$ - see front matter © 2001 Elsevier Science B.V. All rights reserved.
PII: S0169-7722(01)00136-X

32167

Gelhar, 1993; Domenico and Schwartz, 1998; Fetter, 1999). Although many transport problems must be solved numerically, analytical solutions are still pursued by many scientists because they can provide better physical insights into the problems. Analytical solutions are usually derived from the basic physical principles and free from numerical dispersions and other truncation errors that often occurred in numerical simulations (Zheng and Bennett, 1995). With help of analytical solutions to estimate movements of contaminant plumes, we can save a lot of effort to guide and collect data and monitor water quality despite complexities of hydrogeologic systems (Wexler, 1992). Using analytical solutions, we can better understand the mechanism of contaminant transport, predict the movement of contaminant plumes, measure the field parameters related to solute transport, and verify the results of numerical modeling.

The solutions of one-, two-, and three-dimensional deterministic advection–dispersion equations have been investigated in numerous publications before and are still actively studied. For instance, Ogata and Banks (1961), Sauty (1980), and van Genuchten (1981) have provided analytical solutions of one-dimensional transport with the first-type (Dirichlet), second-type (Neumann), and third-type (Cauchy) boundary conditions, respectively. Yeh (1981) have given the generalized analytical one-, two-, and three-dimensional description and computer code for estimating the transport of waste in groundwater aquifers. Domenico and Robbins (1984) and Domenico (1987) have explored some multi-dimensional transport problems.Batu (1989, 1993) have studied the two-dimensional analytical solute transport model with the first- and the second-type boundary conditions. Wexler (1992) and its cited references there have documented many previously derived analytical solutions with different initial and boundary conditions. Leij et al. (1993) have studied the non-equilibrium multi-dimensional transport using the Laplace and Fourier transforms, and Leij et al. (2000) have used Green's functions to describe persistent solute source transport.

Although most of the source bodies of contaminants are usually three-dimensional and finite, the advection–dispersion equation is commonly solved either with an infinitely large source or with a one- or two-dimensional source. A three-dimensional source is rarely considered. Besides that, many of the previous solutions assume that either the sources are fully penetrating through the entire thickness of the aquifer or the aquifers are infinite or semi-infinite along the vertical axis. In reality, aquifers are finite vertically.

Previous works closely related to our study were carried out by Yeh (1981), Domenico and Robbins (1984), Domenico (1987), Batu (1989, 1993), and Leij et al. (2000). Yeh (1981) provided a general framework of using Green's functions to solve transport equations for 450 options without giving too many details. Domenico and Robbins (1984) and Domenico (1987) considered finite sources as boundary conditions when solving the advection–dispersion equation. They did not include the effect from the upper and lower boundaries of an aquifer. Batu (1989, 1993) provided a two-dimensional analytical solute transport model in a bounded aquifer by using the same source dimension as the aquifer thickness along the z-axis and included the contaminant source as a boundary condition. The general solutions were derived there through the help of Fourier analysis and Laplace transform. Leij et al. (2000) also used the Green's function method by including the contaminant source as a boundary condition. In their study, a

vertically semi-infinite aquifer and a vertically infinitely thin source are assumed. In this study, we assume a three-dimensional finite source within a vertically finite-thickness aquifer, and include the source as a source term in the advection–dispersion equation.

The first goal of this paper is using Green's function method to solve the general form of contaminant transport from three-dimensional finite, instantaneous or continuous sources in a finite-thickness aquifer. Using the same methodology, we derive the solutions for the point, line, and area sources in a finite-thickness aquifer. The Green's function method is a convenient way to solve three-dimensional flow and transport problems that include source terms. With a parallelepiped shape of source, the three-dimensional Green's function can be obtained from three separate one-dimensional Green's functions. Such one-dimensional solutions have been provided in previous works (Gringarten and Ramey, 1973).

The second objective of this paper is using the established general methodology to derive various solutions for point, line, and area sources. By generating concentration curves using the derived solutions, we can observe how each of the different source geometries and aquifer conditions influence the concentration distribution. A library of unpublished analytical solutions will be provided.

2. Conceptual and mathematical models

The general geometry of the problem is shown in Fig. 1. The origin of the coordinate system is at the upper boundary. The positive z-axis is downward. The aquifer is assumed infinite in the x- and y-directions but finite in the z-direction with a thickness of d. The aquifer is horizontal without curvature. Bedrock or extremely low-permeability clay stratum exists underneath the aquifer, thus a no-flow boundary is assumed at the bottom of the aquifer ($z = d$). A no-flow or a water table boundary exists at the top of the aquifer. If a water table boundary exists, we assume that the slope of the water table is so small that we can assume the water table to be parallel to the lower boundary. The shape of the contaminant source is a parallelepiped body with, $x \in [0, x_0]$, $y \in [-y_0, y_0]$ and $z \in [z_0, z_1]$. Steady-state groundwater flow is along the x-axis. The three-dimensional deterministic advection–dispersion equation, which describes equilibrium solute transport within a vertically finite aquifer from a finite source, is written as follows:

$$\frac{\partial C}{\partial t} - D_x \frac{\partial^2 C}{\partial x^2} - D_y \frac{\partial^2 C}{\partial y^2} - D_z \frac{\partial^2 C}{\partial z^2} + v \frac{\partial C}{\partial x} + \lambda C = q_v(x, y, z, t) \tag{1}$$

with boundary conditions:

$$C(\pm\infty, y, z, t) = 0, \qquad -\infty < y < \infty, 0 < z < d \text{ and } t > 0 \tag{2}$$

$$C(x, \pm\infty, z, t) = 0, \qquad -\infty < x < \infty, 0 < z < d \text{ and } t > 0 \tag{3}$$

$$\frac{\partial}{\partial z} C(x, y, 0, t) = \frac{\partial}{\partial z} C(x, y, d, t) = 0, \qquad \begin{array}{c} -\infty < x < \infty \\ -\infty < y < \infty \\ t > 0 \end{array} \tag{4}$$

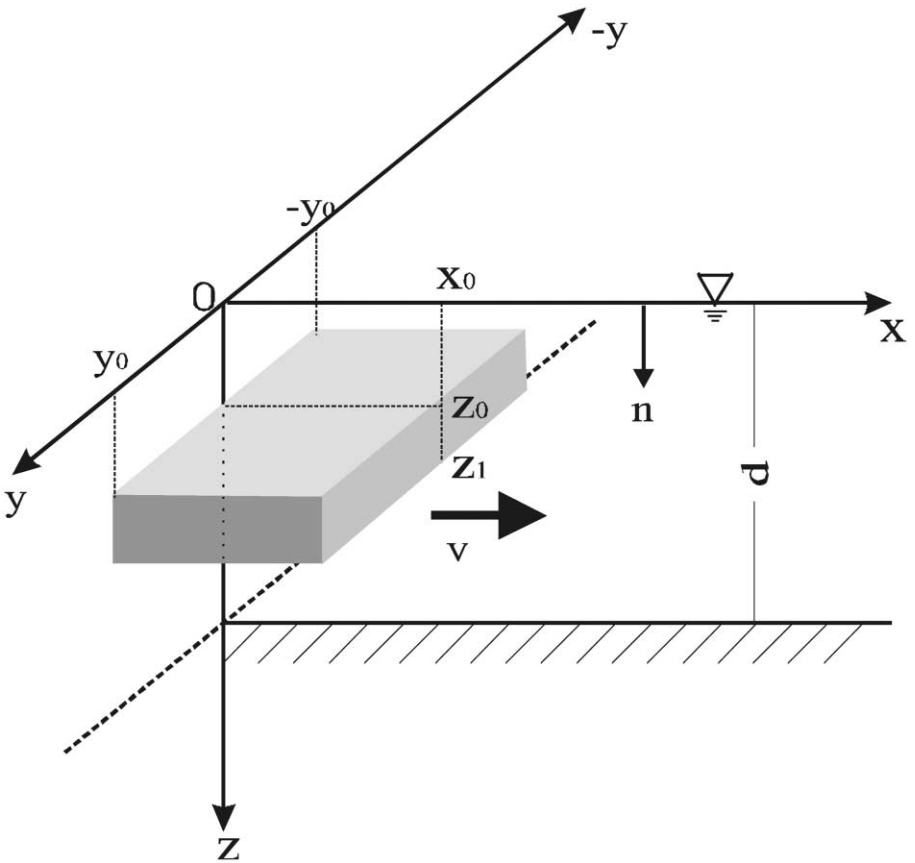

Fig. 1. A schematic diagram of a three-dimensional source body within parallel non-penetrable boundaries for the solute. The upper boundary is a no-flow boundary or a water table boundary. The lower boundary is a no-flow boundary.

and initial condition:

$$C(x,y,z,0) = 0, \qquad \begin{array}{c} -\infty < x < \infty \\ -\infty < y < \infty \\ 0 < z < d \end{array} \tag{5}$$

where C is the solute concentration (kg/m^3); t is time (day); D_x, D_y, and D_z are the principal dispersion coefficients in the x-, y-, and z-directions, respectively (m^2/day); v is the groundwater flow velocity(m/day); λ is the first-order reaction or decay constant (1/day); $q_v(x,y,z,t)$ is the volumetric source strength function (SSF) (kg/(m^3 day)) ($q_v > 0$ means producing contaminant mass, $q_v < 0$ means removing contaminant mass); and d is the thickness of the aquifer (m).

For a three-dimensional finite source, q_v is defined as the mass removed or added to a unit aqueous volume at a unit time interval. q_v is assumed to have the characteristics of Heaviside function (see Fig. 1):

$$q_v(x,y,z,t) = \begin{cases} q_0 f(t), & 0 < x < x_0,\ -y_0 < y < y_0,\ z_0 < z < z_1, \text{and } t > 0 \\ 0 & \text{otherwise} \end{cases} \tag{6}$$

where q_0 is a constant and $f(t)$ is a function of time.

The concentrations at laterally infinite distances are assumed zero. Along the z-direction, both the upper and lower boundaries are assumed non-penetrable for the solute. By transforming x to $\bar{x} = x - vt$, C to $\bar{C} = \exp(\lambda t)C$, q_v to $\bar{q}_v = \exp(\lambda t)q_v$ and doing the following dimensionless transformations:

$$\bar{x}_D = \frac{\bar{x}}{d}\sqrt{\frac{D_z}{D_x}},\ y_D = \frac{y}{d}\sqrt{\frac{D_z}{D_y}},\ z_D = \frac{z}{d},\ t_D = \frac{D_z}{d^2}t,\ \bar{C}_D = \frac{D_z}{q_0 d^2}\bar{C},$$

$$\bar{q}_{vD} = \frac{\bar{q}_v}{q_0},\ v_D = \frac{vd}{\sqrt{D_x D_z}} \tag{7}$$

above Eqs. (1)–(5) become:

$$\frac{\partial \bar{C}_D}{\partial t_D} - \frac{\partial^2 \bar{C}_D}{\partial \bar{x}_D^2} - \frac{\partial^2 \bar{C}_D}{\partial y_D^2} - \frac{\partial^2 \bar{C}_D}{\partial z_D^2} = \begin{cases} \bar{q}_{vD}, & \text{inside the source} \\ 0, & \text{outside the source} \end{cases} \tag{8}$$

$$\bar{C}_D(\pm\infty, y_D, z_D, t_D) = 0, \qquad -\infty < y_D < \infty, 0 < z_D < 1 \tag{9}$$

$$\bar{C}_D(\bar{x}_D, \pm\infty, z_D, t_D) = 0 \qquad -\infty < \bar{x}_D < \infty, 0 < z_D < 1 \tag{10}$$

$$\frac{\partial}{\partial z_D}\bar{C}_D(\bar{x}_D, y_D, 0, t_D) = \frac{\partial}{\partial z_D}\bar{C}_D(\bar{x}_D, y_D, 1, t_D) = 0, \qquad \begin{matrix} -\infty < \bar{x}_D < \infty \\ -\infty < y_D < \infty \end{matrix} \tag{11}$$

$$\bar{C}_D(\bar{x}_D, y_D, z_D, 0) = 0, \qquad \begin{matrix} -\infty < \bar{x}_D < \infty \\ -\infty < y_D < \infty \\ 0 < z_D < 1 \end{matrix} \tag{12}$$

3. Solutions derived using green's function method

3.1. Three-dimensional solutions

Above mathematical model can be solved using Green's function method. Green's function in this problem is defined as the concentration at (x,y,z,t) due to an instantaneous point source of strength unity generated at the point (x', y', z', τ), the aquifer being

initially kept at zero concentration and boundary surface being kept at zero concentration (Gringarten and Ramey, 1973). This method has been used in fewer previous studies of contaminant transport (Yeh, 1981; Leij et al., 2000). Detailed description of the Green's function method can be found from Carslaw and Jaeger (1959), Gringarten and Ramey (1973), and Arfken and Weber (1995).

The Green's function of this problem can be obtained by solving the following differential equation with initial and boundary conditions (Eqs. (9)–(12)).

$$\frac{\partial^2 G}{\partial \bar{x}_D^2} + \frac{\partial^2 G}{\partial y_D^2} + \frac{\partial^2 G}{\partial z_D^2} - \frac{\partial G}{\partial t_D} = \delta(\bar{x}_D - \bar{x}'_D)\,\delta(y_D - y'_D)\,\delta(z_D - z'_D)\,\delta(t_D - t'_D) \tag{13}$$

The three-dimensional Green's function can be expressed as the product of three one-dimensional Green's functions. The one-dimensional Green's function in an infinite aquifer is (Carslaw and Jaeger, 1959):

$$G(j_D, j'_D, t_D) = \frac{1}{2\sqrt{\pi t_D}} \exp\left(-\frac{(j_D - j'_D)^2}{4t_D}\right),\ j = \bar{x}, y \text{ or } z \tag{14}$$

where, j'_D and j_D denote the coordinates of the source point and measured point, respectively.

The Green's function method is commonly applied using the source function (SF), which is defined as the integration of the Green's function over the volume or area or length of the source (Carslaw and Jaeger, 1959; Gringarten and Ramey, 1973). Using the Green's function method, the concentration in Eq. (8) can be written as follows (Carslaw and Jaeger, 1959; Gringarten and Ramey, 1973):

$$\begin{aligned}\bar{C}_D(\bar{x}_D, y_D, z_D, t_D) &= \int_0^{t_D} \bar{q}_D(\tau_D) \int_\Omega G(\bar{x}_D, y_D, z_D, t_D - \tau_D; \bar{x}'_D, y'_D, z'_D)\,\mathrm{d}\Omega\,\mathrm{d}\tau_D \\ &= \int_0^{t_D} \bar{q}_D(\tau_D)\, S(\bar{x}_D, y_D, z_D, t_D - \tau_D)\,\mathrm{d}\tau_D \end{aligned} \tag{15}$$

where Ω is the source domain, G is the Green's function, and S is the source function.

Eq. (15) shows that the continuous source solution is simply the temporal convolution of the source strength function $\bar{q}_D$ and the source function S. Applying Neumann's product rule, the three-dimensional source function is expressed as the product of three one-dimensional source functions:

$$S(\bar{x}_D, y_D, z_D, t_D - \tau_D) = S(\bar{x}_D, t_D - \tau_D)\, S(y_D, t_D - \tau_D)\, S(z_D, t_D - \tau_D) \tag{16}$$

Through the z-axis, the one-dimensional source function, $S(z_D, t_D - \tau_D)$, is represented as an integration of the one-dimensional Green's function, $G(z_D, z'_D, t_D - \tau_D)$, from z_{0D} to z_{1D}, where z_{0D} and z_{1D} are the dimensionless source dimensions in the z-direction, defined in Eq. (7). Along the vertical direction, there are two boundaries that contami-

nant cannot penetrate through. To solve the boundary value problem, the method of image is applied (Bear, 1972). The method of image uses infinite numbers of image sources along the z-axis to replace the upper and lower boundaries (Zhan, 1999). The source function along the z-axis is a summation of the source function of the original source and the source functions of all the image sources. The resulting source function in the z-axis is given by Eq. (17) (Carslaw and Jaeger, 1959, p. 275).

$$S(z_D, t_D - \tau_D) = \int_{z_{0D}}^{z_{1D}} \left[1 + 2\sum_{n=1}^{\infty} \cos n\pi\zeta_D \cos n\pi z_D \exp\left[-n^2\pi^2(t_D - \tau_D)\right] \right] d\zeta \tag{17}$$

Through the y-axis, the source function is an integration of the corresponding one-dimensional Green's function from $-y_{0D}$ to y_{0D} along the y-axis (Gringarten and Ramey, 1973):

$$S(y_D, t_D - \tau_D) = \frac{1}{2\sqrt{\pi(t_D - \tau_D)}} \int_{-y_{0D}}^{y_{0D}} \exp\left[-\frac{(y_D - \psi_D)^2}{4(t_D - \tau_D)} \right] d\psi_D \tag{18}$$

where y_{0D} is the dimensionless y_0 defined in Eq. (7).

The source function along the x-axis is derived as follows. The source along the $\bar{x}_D$-axis is between $-v_D\tau_D$ and $x_{0D} - v_D\tau_D$ in the coordinate system $(\bar{x}_D, y_D, z_D)$ at time τ_D. Notice that the source function $S(\bar{x}_D, t_D - \tau_D)$ is referred to an instantaneous source at time τ_D and it is the spatial integration of the corresponding Green's function at that time τ_D. Thus, when calculating $S(\bar{x}_D, t_D - \tau_D)$, τ_D is treated as a fixed value. Therefore, $S(\bar{x}_D, t_D - \tau_D)$ is (Gringarten and Ramey, 1973):

$$S(\bar{x}_D, t_D - \tau_D) = \frac{1}{2\sqrt{\pi}} \int_{-v_D\tau_D}^{x_{0D} - v_D\tau_D} \frac{1}{\sqrt{t_D - \tau_D}} \exp\left[-\frac{(\bar{x}_D - \xi_D)^2}{4(t_D - \tau_D)} \right] d\xi_D \tag{19}$$

The ultimate solution of our problem is given by the integration of product of Eqs. (17)–(19).

$$\begin{aligned} &\bar{C}_D(\bar{x}_D, y_D, z_D, t_D) \\ &\quad = \frac{1}{4\pi} \int_0^{t_D} \bar{q}_{vD}(\tau_D) \int_{-v_D\tau_D}^{x_{0D} - v_D\tau_D} \int_{-y_{0D}}^{y_{0D}} \int_{z_{0D}}^{z_{1D}} \frac{1}{t_D - \tau_D} \\ &\qquad \times \exp\left[-\frac{(\bar{x}_D - \xi_D)^2 + (y_D - \psi_D)^2}{4(t_D - \tau_D)} \right] \\ &\qquad \times \left[1 + 2\sum_{n=1}^{\infty} \cos n\pi\zeta_D \cos n\pi z_D \exp\left[-n^2\pi^2(t_D - \tau_D)\right] \right] d\xi_D\, d\psi_D\, d\zeta_D\, d\tau_D \end{aligned} \tag{20}$$

Changing the integration parameter from τ_D to $\tau'_D = t_D - \tau_D$ in Eq. (20) and finishing the spatial integration first, we have:

$$\begin{aligned}
&\bar{C}_D(\bar{x}_D, y_D, z_D, t_D) \\
&\quad = \frac{1}{4}\int_0^{t_D} \bar{q}_{vD}(t_D - \tau'_D) \\
&\qquad \times \left[\operatorname{erfc}\frac{\bar{x}_D - x_{0D} + v_D(t_D - \tau'_D)}{2\sqrt{\tau'_D}} - \operatorname{erfc}\frac{\bar{x}_D + v_D(t_D - \tau'_D)}{2\sqrt{\tau'_D}}\right] \\
&\qquad \times \left[\operatorname{erfc}\frac{y_D - y_{0D}}{2\sqrt{\tau'_D}} - \operatorname{erfc}\frac{y_D + y_{0D}}{2\sqrt{\tau'_D}}\right] \\
&\qquad \times \left[z_{1D} - z_{0D} + \frac{2}{\pi}\sum_{n=1}^{\infty}\frac{1}{n}(\sin n\pi z_{1D} - \sin n\pi z_{0D})\cos n\pi z_D\right. \\
&\qquad \left. \times \exp\left[-n^2\pi^2\tau_D\right]\right] d\tau'_D
\end{aligned} \tag{21}$$

If expressed in a dimensional format, Eq. (21) becomes:

$$\begin{aligned}
C(x,y,z,t) = \frac{1}{4d}\int_0^t q_v(t-\tau')\exp(-\lambda\tau')&\left[\operatorname{erfc}\frac{x - v\tau' - x_0}{2\sqrt{D_x\tau'}} - \operatorname{erfc}\frac{x - v\tau'}{2\sqrt{D_x\tau'}}\right] \\
&\times\left[\operatorname{erfc}\frac{y - y_0}{2\sqrt{D_y\tau'}} - \operatorname{erfc}\frac{y + y_0}{2\sqrt{D_y\tau'}}\right] \\
&\times\left[z_1 - z_0 + 2\sum_{n=1}^{\infty}\frac{d}{n\pi}\left(\sin\frac{n\pi z_1}{d} - \sin\frac{n\pi z_0}{d}\right)\cos\frac{n\pi z}{d}\right. \\
&\left.\times\exp\left[-\left(\frac{D_z n^2\pi^2}{d^2}\right)\tau'\right]\right]d\tau'
\end{aligned} \tag{22}$$

Eqs. (21) and (22) are the dimensionless and dimensional solutions of contaminant transport in a finite-thickness aquifer with a three-dimensional finite source.

If an instantaneous source exists, the SSF $q_v(t) = C_0\,\delta(t)$, where C_0 is the source concentration at time t, and $\delta(t)$ is the Dirac Delta function. Therefore, the instantaneous source solution is expressed by the same equation as Eq. (22) without doing the integration and q_v is replaced by C_0. If the source is eliminated at a certain time t', we can get the solution by changing the lower limit of the integration from 0 to $t - t'$ in Eq. (22).

It is important to emphasize the physical conditions, applications, and limitations of Eq. (22) in order to make use of this formula for practical purpose:

(1) This equation calculates concentrations for reactive solute transport in a vertically finite but horizontally infinite, homogeneous, and anisotropic aquifer with a three-di-

mensional parallelepiped source body $x \in [0, x_0]$, $y \in [-y_0, y_0]$, and $z \in [z_0, z_1]$. The first-order reaction or radioactive decay has been taken into account. The linear sorption can be incorporated by replacing v, D_x, D_y, and D_z with v/R, D_x/R, D_y/R, and D_z/R, respectively, where R is the retardation factor. A time-dependent but space-independent source strength function is used. If the source strength function depends on both time and space, $\bar{q}_D(\tau)$ in Eq. (15) should be replaced by $\bar{q}_D(\tau, \bar{x}'_D, y'_D, z'_D)$ and it cannot be taken out of the spatial integration in Eq. (15).

(2) The initial concentration is assumed zero in Eq. (22). If a non-zero initial concentration C_i exists, one additional term $\int_\Omega (C_i G) \mathrm{d}\Omega$ should be added in Eq. (15).

(3) The following discussion explains how to determine q_v and source concentration C_0 at some hypothetical cases. If doing a tracer test with a continuously adding tracer, q_v is the amount of mass added to the source zone per unit volume of pore water per unit time. If doing a tracer test with an instantaneous tracer, C_0 is the mass of tracer added to the source zone per unit volume of pore water per unit time. If free phase contaminants such as LNAPLs and DNAPLs exist in the aquifer, then dissolved free phase contaminants become the sources of aqueous phase contamination. The dissolution process cannot be easily handled by solution (22) because of the difficulty of accurately determining the source strength function. However, that process can be handled by Leij et al. (2000) solution if treating the source as a boundary condition rather than a source term inside the studied domain.

(4) The molecular diffusion into the upper and lower boundaries is not considered in this paper in order to derive the analytical solutions. By neglecting the molecular diffusion, we will slightly overestimate the concentration in the aquifer when time is so long that the contaminant plume reaches the boundaries.

3.2. One- and two-dimensional solutions

Using Eq. (22) as a base, a library of analytical solutions for different source types are derived and shown in Table 1. The source types in Table 1 include a point source (Case A, Fig. 2a), three line sources (Cases B–D, Fig. 2b–d), and two area sources (Cases E–F, Fig. 2e–f).

The SSF for a point case, denoted as q_p, is defined as the produced or removed mass per unit time at the point [M/T]; the SSF for a line source, denoted as q_l, is defined as the produced or removed mass per unit length per unit time [M/(LT)]; and the SSF for an area source, denoted as q_a, is defined as the produced or removed mass per unit area per unit time [M/(L^{2}T)].

The point source in Fig. 2a is at $(0,0,z_0)$. The sources in Fig. 2b–d are line sources with infinitesimal radius. The source in Fig. 2b spans along the x-direction, from $(0,0,z_0)$ to $(x_0,0,z_0)$, parallel to the groundwater flow. The source in Fig. 2c spans along the y-direction, from $(0,-y_0,z_0)$ to $(0,y_0,z_0)$, normal to the groundwater flow. The source in Fig. 2d spans along the z-direction, from $(0,0,z_0)$ to $(0,0,z_1)$, normal to the groundwater flow. The sources in Fig. 2e and f are rectangular area sources. The source in Fig. 2e is on the yz-plane with infinitesimal thickness along the x-direction; it is from $-y_0$ to y_0 along the y-direction and from z_0 to z_1 along the z-direction. The

Table 1
Solutions of several general types of sources: Case A is a point source; Cases B–D are the line sources with different positions; and Cases E–F are the area sources with different positions

Solution of given geometry		Source type
$C(x,y,z,t)=\frac{1}{4d\pi\sqrt{D_xD_y}}\int_0^t q_p(t-\tau)\exp(-\lambda\tau)\exp\left[-\frac{(x-v\tau)^2}{4D_x\tau}\right]\times\exp\left[-\frac{y^2}{4D_y\tau}\right]$	Case A	point source
$\times\left[1+2\sum_{n=1}^{\infty}\cos\frac{n\pi z_0}{d}\cos\frac{n\pi z}{d}\exp\left[-\frac{D_z n^2\pi^2}{d^2}\tau\right]\right]\frac{d\tau}{\tau}$		(Fig. 2a)
$C(x,y,z,t)=\frac{1}{4d\sqrt{D_y\pi}}\int_0^t q_l(t-\tau)\exp(-\lambda\tau)\left[\mathrm{erfc}\frac{x-v\tau-x_0}{2\sqrt{D_x\tau}}-\mathrm{erfc}\frac{x-v\tau}{2\sqrt{D_x\tau}}\right]\times\exp\left[-\frac{y^2}{4\tau D_y}\right]$	Case B	line source
$\times\left[1+2\sum_{n=1}^{\infty}\cos\frac{n\pi z_0}{d}\cos\frac{n\pi z}{d}\exp\left[-\frac{D_z n^2\pi^2}{d^2}\tau\right]\right]\frac{d\tau}{\sqrt{\tau}}$		(Fig. 2b)
$C(x,y,z,t)=\frac{1}{4d\sqrt{D_x\pi}}\int_0^t q_l(t-\tau)\exp(-\lambda\tau)\exp\left[-\frac{(x-v\tau)^2}{4D_x\tau}\right]\times\left[\mathrm{erfc}\frac{y+y_0}{2\sqrt{D_y\tau}}-\mathrm{erfc}\frac{y-y_0}{2\sqrt{D_y\tau}}\right]$	Case C	line source
$\times\left[1+2\sum_{n=1}^{\infty}\cos\frac{n\pi z_0}{d}\cos\frac{n\pi z}{d}\exp\left[-\frac{D_z n^2\pi^2}{d^2}\tau\right]\right]\frac{d\tau}{\sqrt{\tau}}$		(Fig. 2c)

$C(x,y,z,t)=\frac{1}{4d\pi\sqrt{D_xD_y}}\int_0^t q_l(t-\tau)\exp(-\lambda\tau)\exp\left[-\frac{(x-v\tau)^2}{4D_x\tau}\right]\times\exp\left[-\frac{y^2}{4D_y\tau}\right]$	Case D	line source
$\times\left[z_1-z_0+\frac{2d}{\pi}\sum_{i=1}^{\infty}\frac{1}{n}\left(\sin\frac{n\pi z_1}{d}-\sin\frac{n\pi z_0}{d}\right)\cos\frac{n\pi z}{d}\exp\left[-\frac{D_z n^2\pi^2}{d^2}\tau\right]\right]\frac{d\tau}{\tau}$		(Fig. 2d)
$C(x,y,z,t)=\frac{1}{4d\sqrt{D_x\pi}}\int_0^t q_a(t-\tau)\exp(-\lambda\tau)\exp\left[-\frac{(x-v\tau)^2}{4D_x\tau}\right]\times\left[\mathrm{erfc}\frac{y+y_0}{2\sqrt{D_y\tau}}-\mathrm{erfc}\frac{y-y_0}{2\sqrt{D_y\tau}}\right]$	Case E	area source
$\times\left[z_1-z_0+\frac{2}{\pi}\sum_{n=1}^{\infty}\frac{1}{n}\left(\sin\frac{n\pi z_1}{d}-\sin\frac{n\pi z_0}{d}\right)\cos\frac{n\pi z}{d}\exp\left[-\frac{D_z n^2\pi^2}{d^2}\tau\right]\right]\frac{d\tau}{\sqrt{\tau}}$		(Fig. 2e)
$C(x,y,z,t)=\frac{1}{4d}\int_0^t q_a(t-\tau)\exp(-\lambda\tau)\left[\mathrm{erfc}\frac{x-x_0-v\tau}{2\sqrt{D_x\tau}}-\mathrm{erfc}\frac{x-v\tau}{2\sqrt{D_x\tau}}\right]$	Case F	area source
$\times\left[\mathrm{erfc}\frac{y+y_0}{2\sqrt{D_y\tau}}-\mathrm{erfc}\frac{y-y_0}{2\sqrt{D_y\tau}}\right]\times\left[1+2\sum_{n=1}^{\infty}\cos\frac{n\pi z_0}{d}\cos\frac{n\pi z}{d}\exp\left[-\frac{D_z n^2\pi^2}{d^2}\tau\right]\right]d\tau$		(Fig. 2f)

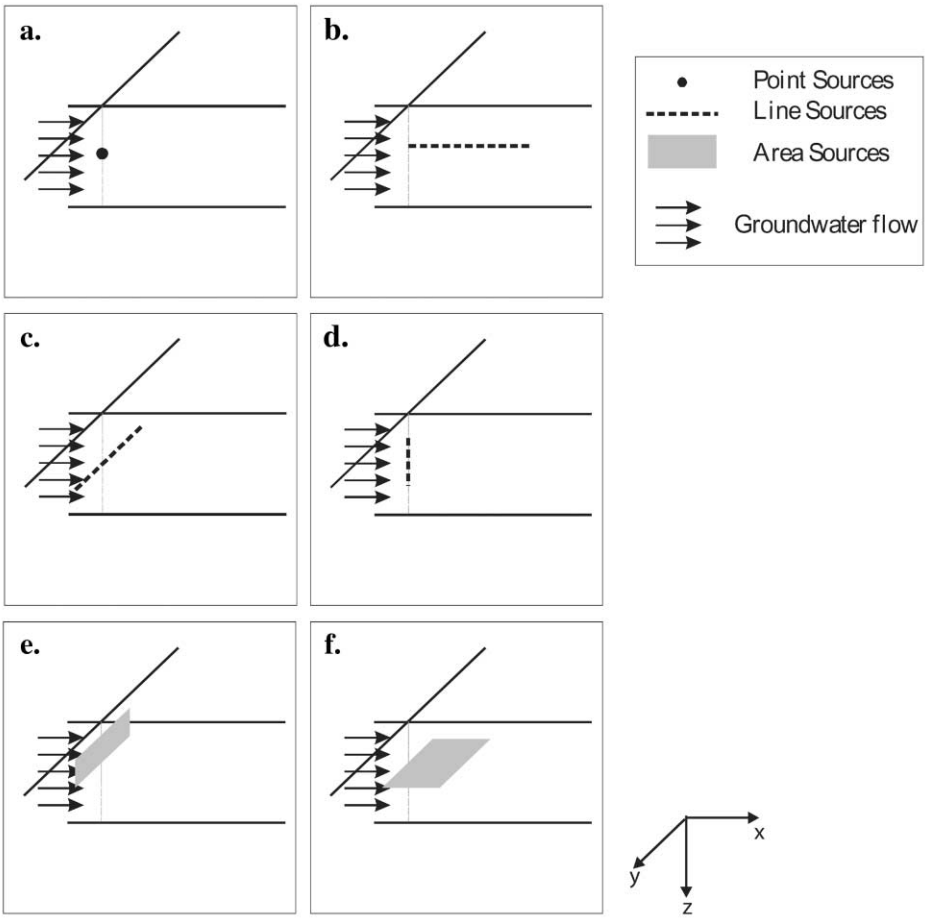

Fig. 2. Schematic diagrams of various source shapes within two parallel non-penetrable boundaries for the solute. (a) A point source; (b) a horizontal line source parallel to the regional flow; (c) a horizontal line source perpendicular to the regional flow; (d) a vertical line source perpendicular to the regional flow; (e) an area source perpendicular to the regional flow; and (f) an area source parallel to the upper and lower boundaries.

source in Fig. 2f is located on the xy-plane with a distance z_0 below the upper boundary; it is from $-y_0$ to y_0 along the y-direction and from 0 to x_0 along the x-direction.

Eq. (22) can be simplified in certain special cases. For instances, if the source dimension in the vertical direction is the same as the aquifer thickness, the solution becomes independent of the vertical coordinate. If the source dimension in the y-direction is infinite, then the solution is independent of the y-coordinate. Through these manipulations, the general solution (22) will converge to some typical solutions derived before by other investigators (Morgenau and Murphy, 1956; Ogata and Banks, 1961; Leij et al., 2000). Time-dependent source strength function can be applied to the solution

to simulate the loading history of the contaminant sources. Some typical cases are discussed below and their results are compared with previous solutions.

Case 1 (A continuous area source located at the upper boundary in a semi-infinite aquifer). In this special case, the continuous source has an infinitesimal thickness along the z-direction; an extension from 0 to x_0 along the x-direction; and an extension from $-y_0$ to y_0 along the y-direction. The source is located at the upper boundary. The lower impermeable boundary is assumed to be far from the source thus its influence upon the transport is negligible. Therefore, the source function along the z-direction becomes:

$$S(z,t) = \frac{1}{\sqrt{\pi D_z \tau}} \exp\left(-\frac{z^2}{4D_z\tau}\right) \tag{23}$$

If including the first-order decay, the concentration then becomes:

$$\begin{aligned} C(x,y,z,t) &= \frac{1}{4\sqrt{\pi D_z}} \int_0^t q(t-\tau) \exp\left(-\lambda\tau - \frac{z^2}{4D_z\tau}\right) \left[\operatorname{erfc}\frac{x - v\tau - x_0}{2\sqrt{D_x\tau}} - \operatorname{erfc}\frac{x - v\tau}{2\sqrt{D_x\tau}}\right] \\ &\quad \times \left[\operatorname{erfc}\frac{y - y_0}{2\sqrt{D_y\tau}} - \operatorname{erfc}\frac{y + y_0}{2\sqrt{D_y\tau}}\right] \frac{d\tau}{\sqrt{\tau}} \end{aligned} \tag{24}$$

Eq. (24) is identical to the equation of the second type source solution given by Leij et al. (2000, p.166, Eq. (24)) but $q(t-\tau)$ is replaced by the mass flux, $D_z((\partial C)/(\partial z))$ at $z = 0$, given by Fick's law in their equation. Notice that the y- and z-axes used in Leij et al. (2000, Fig. 1 there) are equivalent to the z- and y-axes in our coordinate system, respectively (Fig. 1).

Case 2 (A fully penetrated instantaneous source). If we extend the source length along the z-axis to the aquifer thickness and exclude the first-order decay and sorption,

$$S(z,t) = \frac{1}{d}\left[d + 2\sum_{n=1}^{\infty} \frac{d}{n\pi} \sin\frac{n\pi d}{d} \cos\frac{n\pi z}{d} \exp\left[-\frac{D_z n^2 \pi^2 t}{d^2}\right]\right] = 1 \tag{25}$$

For a problem with an instantaneous source, $q_v(t) = C_0\,\delta(t)$. Eq. (22) becomes Eq. (26).

$$C(x,y,t) = \frac{C_0}{4}\left[\operatorname{erfc}\frac{x - vt}{2\sqrt{D_x t}} - \operatorname{erfc}\frac{x - vt - x_0}{2\sqrt{D_x t}}\right]\left[\operatorname{erfc}\frac{y + y_0}{2\sqrt{D_y t}} - \operatorname{erfc}\frac{y - y_0}{2\sqrt{D_y t}}\right] \tag{26}$$

Eq. (26) agrees with the two-dimensional solution derived by Morgenau and Murphy (1956).

Case 3 (An instantaneous semi-infinite source). For a problem with an instantaneous source, if we extend the source length along the z-axis to the aquifer thickness, the source length along the y-axis to infinity, the source length along the x-axis from 0 to negative infinity, and exclude the first-order decay and sorption, we can reproduce the solution derived by Ogata and Banks (1961). In this case:

$$S(y,t) = \frac{1}{2}\left[\operatorname{erfc}\frac{y-\infty}{2\sqrt{D_y t}} - \operatorname{erfc}\frac{y+\infty}{2\sqrt{D_y t}}\right] = 1 \tag{27}$$

$$S(x,t) = \frac{1}{2}\left[\operatorname{erfc}\frac{x-vt}{2\sqrt{D_x t}} - \operatorname{erfc}\frac{x-vt+\infty}{2\sqrt{D_x t}}\right] = \frac{1}{2}\operatorname{erfc}\frac{x-vt}{2\sqrt{D_x t}} \tag{28}$$

Therefore, Eq. (22) becomes Eq. (29), which is the well-known Ogata and Banks' solution (Ogata and Banks, 1961; Domenico and Schwartz, 1998).

$$C(x,y,z,t) = \frac{C_0}{2}\operatorname{erfc}\frac{x-vt}{2\sqrt{D_x t}} \tag{29}$$

where C_0 is the concentration of the source.

3.3. Numerical calculation of the concentration

The analytical solutions shown in above Eq. (22) and in Table 1 include the temporal integrations. A numerical integration program using the Gaussian Quadrature method (Abramowitz and Stegun, 1972) is written in a MATLAB® M-file (MathWorks, 2000). A visual graphical interface is built in the program so that input and output handling becomes straightforward. This program has the following characteristics.

1. It can calculate concentration at any given time for any given type of sources presented in Figs. 1 and 2.
2. It can calculate concentration for both continuous and instantaneous sources including the first-order decay.
3. It can automatically calculate the abscissas and weights used in the Gaussian Quadrature to achieve the desired accuracy of integration.

4. Characteristics and applications of the solutions

4.1. Characteristics and applications of the three-dimensional solution

The results of this study have many applications. For instance, Eq. (22) can be directly applied to sources located within or on the boundaries. Typical cases of this kind could be a smear zone of a chemical spill, formed by a changing water table, or a

leaking landfill. The solutions for the line sources can be applied to wells, abandoned mines, utility pipes, ditches, etc.

Fig. 3 shows the results of a contaminant plume caused by a source similar to a smear zone of a continuous chemical spill, calculated from Eq. (22) using the numerical program described above. Two cases are presented here for comparison. Fig. 3a–b is the results in a finite-thickness aquifer in which the lower boundary is at $z = d$, Fig. 3c–d is the results in a semi-infinite aquifer in which the lower boundary is at $z = \infty$. As expected, the plume spreads out with time and the plume movement depends on the

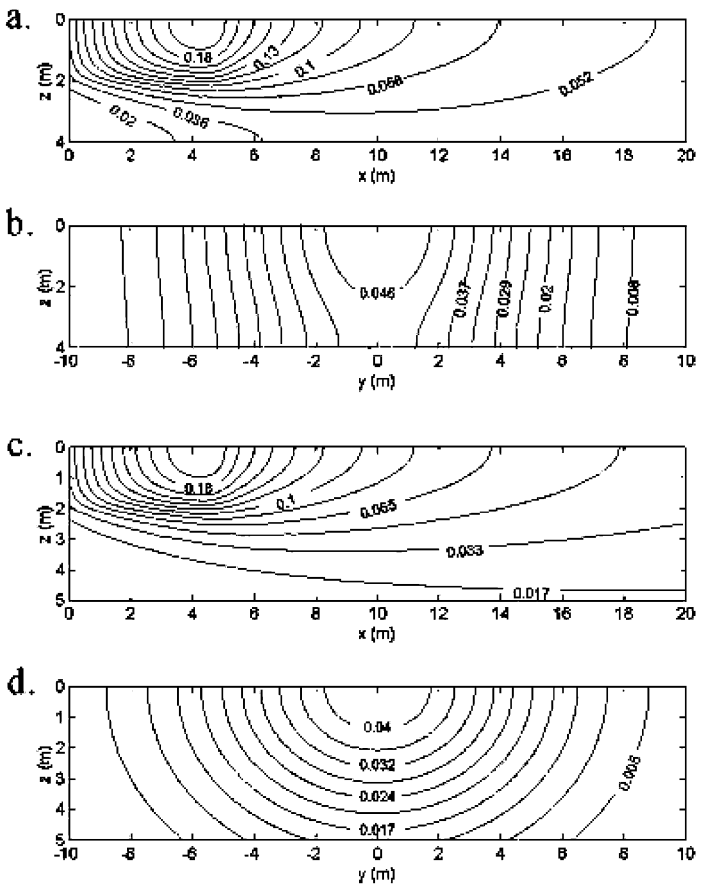

Fig. 3. Iso-concentration contours on the xz-plane ($y = 0$) and yz-plane ($x = 20$ m) in 2 years after injecting of solute. The source strength is $q_v = 0.01$ g/(m^3 day). The source dimensions are $x \in [0, x_0]$, $y \in [-y_0, y_0]$, and $z \in [0, z_0]$ where $x_0 = 5$, $y_0 = 1$, and $z_0 = 2$ m. The aquifer parameters are $d = 5$ m, $D_x = 0.1$ m^2/d, $D_y / D_x = 0.5$, and $D_z / D_x = 0.3$. (a) xy-slice plane passing through the center of the source along the z-axis in a finite-thickness aquifer; (b) yz-slice plane passing through $x = 20$ m in a finite-thickness aquifer; (c) xy-slice plane passing through the center of the source along the z-axis in a semi-infinite aquifer.; and (d) yz-slice plane passing through $x = 20$ m in a semi-infinite aquifer.

regional flow velocity. The degree of spreading depends on the dispersion coefficients of each direction. Because the source is closer to the upper boundary, the expansion of the plume along the $+z$-direction is prohibited. The iso-concentration profiles in Fig. 3b are perpendicular to the upper and lower boundaries, reflecting the influence of impermeable conditions at $z=0$ and $z=d$. The iso-concentration profiles in Fig. 3d are semi-elliptic shapes, reflecting the impermeable condition at $z=0$ and an infinitely far lower boundary.

Domenico and Schwartz (1998, p. 379) also discussed the influence of a finite aquifer thickness upon the evolution of a plume. They gave an order-of-magnitude estimation of the distance at which the plume will "touch" the lower boundary. The Eq. (22) in this paper is a rigorous solution including the influence of the upper and lower boundaries upon the concentration.

4.2. Effects of source geometry, dispersion coefficients, and distance from the source

Figs. 4 and 5 show the influence of source geometry and dispersion coefficients on the concentration distribution. Fig. 6 shows the influence of distance from the source on the concentration distribution. Three line sources are included in Figs. 4–6.

The following parameters are used in Figs. 4–6. The source mass per unit length is 0.09 g/m for the instantaneous line source in Fig. 4. The source strength function q_1 is 0.09 (g/(m day)) for the continuous line source in Fig. 5. The line source along the x-axis is from (0,0,8 m) to (8 m,0,8 m); the line source along the y-axis is from (0, − 4 m,8 m) to (0,4 m,8 m); and the line source along the z-axis is from (0,0,0) to (0,0,8 m).

The concentration profiles of instantaneous sources in Fig. 4 show left skewed bell shapes. This is consistent with what was found before for a finite-length source in the x-direction (Zhan, 1998). Such left skewed bell shapes are caused by the subtraction of two x-dependent complementary error functions in Eq. (22) and in Table 1. If $x_0 \to 0$, the skewed bell shapes will become symmetric bell shapes.

As shown in Figs. 4a and 5a, difference of the source geometry affects the concentration distribution significantly if dispersion coefficients are anisotropic. The horizontal line source along the regional flow shows the highest concentration, the horizontal line source normal to the regional flow shows the second highest concentration, and the vertical source shows the lowest concentration. If $D_x = D_y = D_z$, Figs. 4b and 5b show that the difference of the source geometry has less significant influence upon the concentration distributions.

When the dispersion coefficients are isotropic, the differences of concentration distributions are less significant for different line source orientations. The remaining slight differences in Figs. 4b and 5b are caused by the finite aquifer dimensions in the z-direction. If the aquifer thickness is infinite, those differences will disappear.

Figs. 4 and 5 indicate that the source geometry has a profound influence on the concentration profiles when the dispersion coefficients are anisotropic. Such influence is insignificant when the dispersion coefficients are isotropic.

Fig. 6 is similar to Fig. 5b except that the measuring point is 50-m downstream in Fig. 6, while it is 20-m downstream in Fig. 5b. Comparison of Figs. 5b and 6 shows that

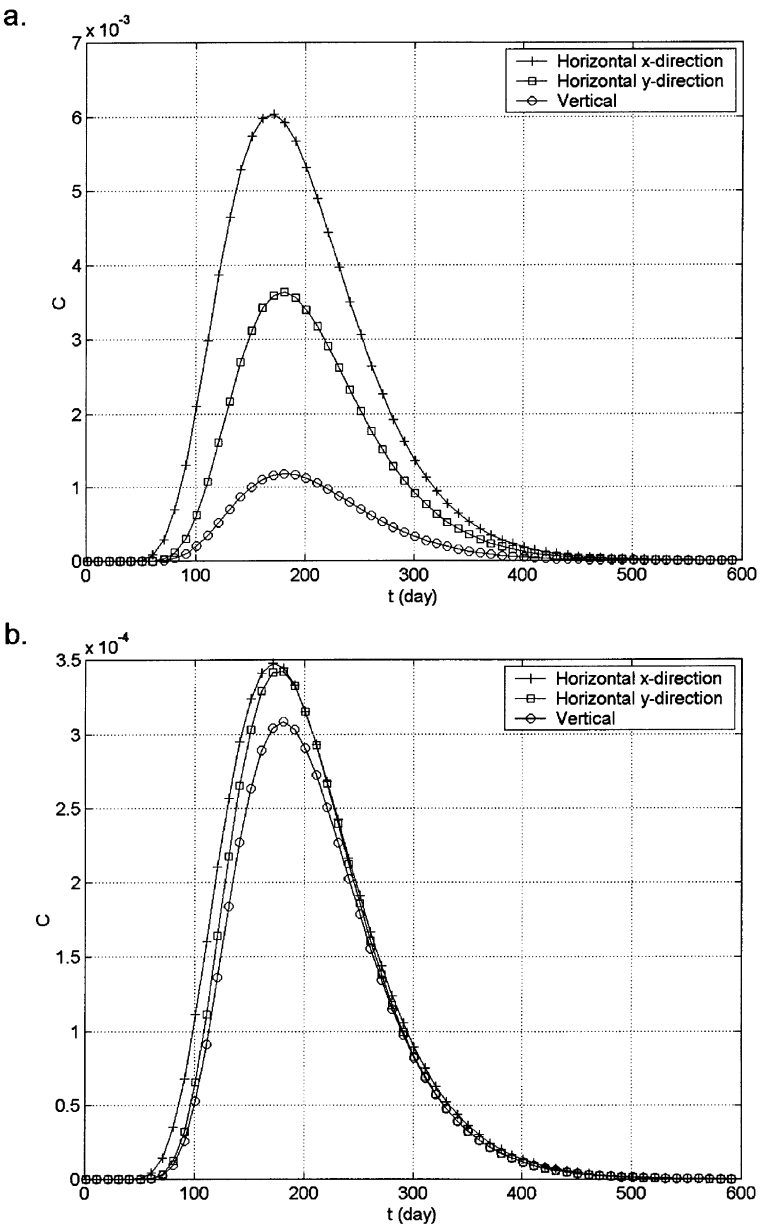

Fig. 4. Theoretical concentration measured at 20-m downstream from the center of the sources that is released instantaneously. The released mass per unit length of the source $C_0 = 0.09$ g/m, $D_x = 0.1$ m^2/d, $d = 10$ m. (a) Comparison of concentrations from three different types of sources, the ratio of D_y / D_x and D_z / D_x are 0.1 and 0.01, respectively; (b) comparison of concentrations from three different types of sources, the ratio of D_y / D_x and D_z / D_x are all 1.

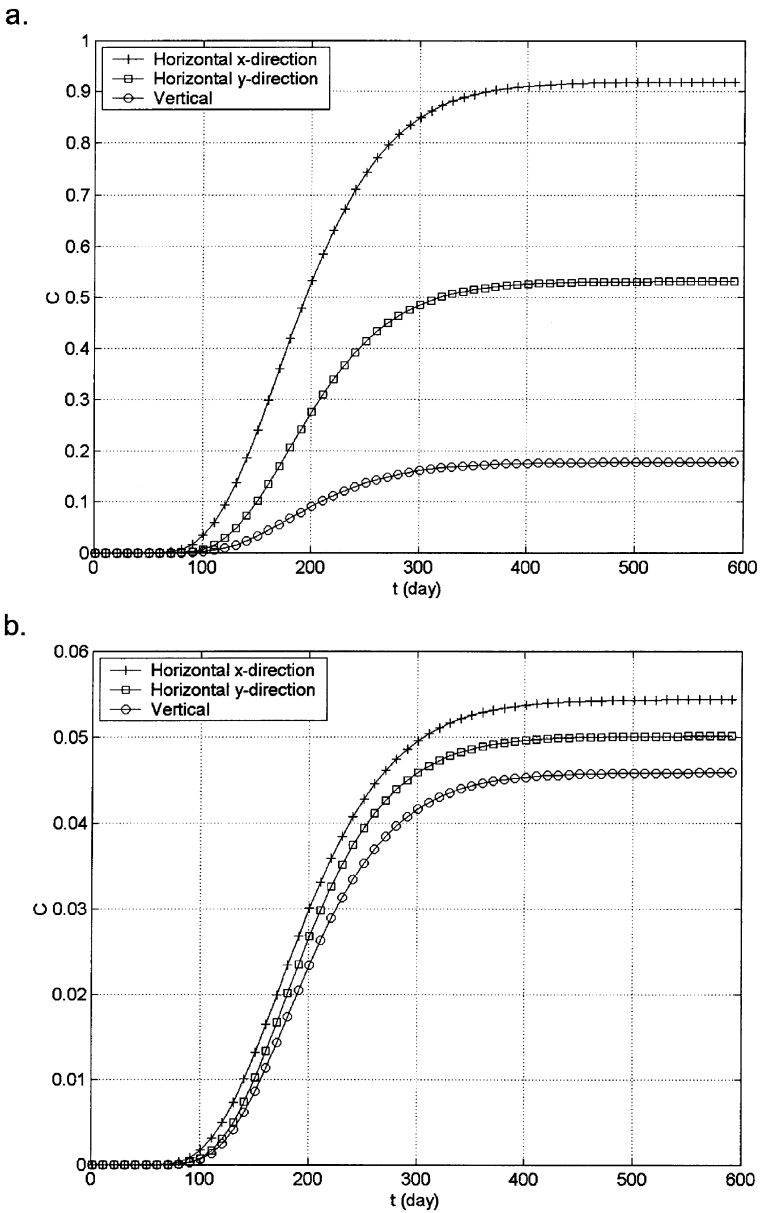

Fig. 5. Theoretical concentration measured at 20-m downstream from the center of the line sources that is released continuously where $q_1 = 0.09$ g/(m day), $D_x = 0.1$ m^2/day, and $d = 10$ m. (a) Comparison of concentrations from three different types of line sources, the ratio of D_y / D_x and D_z / D_x are 0.1 and 0.01, respectively; (b) comparison of concentrations from three different types of line sources, the ratio of D_y / D_x and D_z / D_x are all 1.

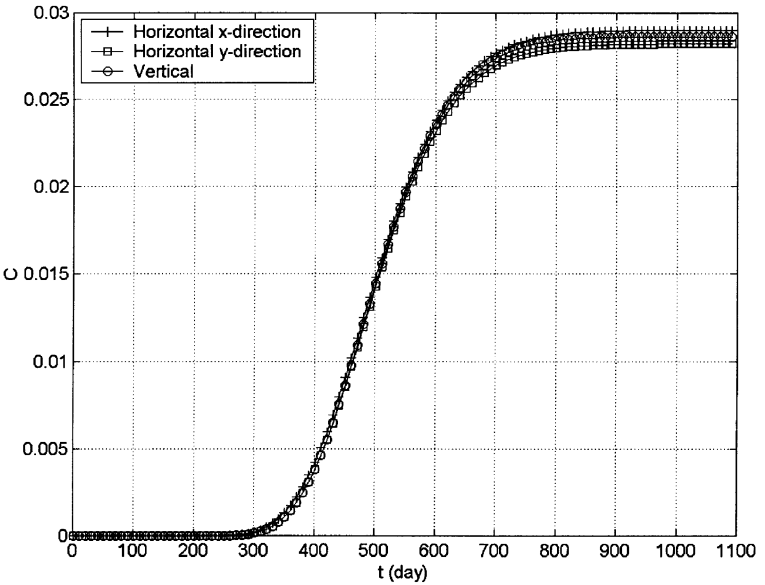

Fig. 6. Comparison of the theoretical concentration measured at 50 m downstream from the center of the source with three different types of continuous line sources. $q_l = 0.09$ g/(m day), $D_x = 0.1$ m^2/d, $d = 10$ m, the ratio of D_y/D_x and D_z/D_x are all 1.

at a near field point (Fig. 5b), the source geometry influences the concentration distribution, but at a far field point (Fig. 6), the source geometry has an almost negligible influence upon the concentration distribution.

5. Summary and conclusions

We generated analytical solutions of multi-dimensional concentration fields originated from one-, two-, and three-dimensional, finite sources within finite-thickness aquifers using the Green's function method. Our solution is examined by reproducing the special solutions of previous works. Based on the general three-dimensional solutions (Eq. (22)), a library of analytical solutions for different source shapes is published in Table 1. The temporal integrations in the analytical solutions are calculated using a graphically integrated MATLAB® program. The program is available from the author's website http://geoweb.tamu.edu/Faculty/Zhan/Research.html.

The derived analytical solutions show that the upper and lower aquifer boundaries have a profound influence upon the concentration distribution. We also find that the concentration at a near field point is sensitive to the source geometry when the dispersion coefficients are anisotropic; it is less sensitive to the source geometry when the dispersion coefficients are isotropic. The concentration at a far field is found to be almost independent of the source geometry.

The limitation of these analytical solutions is that they assume simplified aquifer geometry with no slope and a uniform one-dimensional groundwater flow. Molecular

diffusion into the upper and lower no-flow boundaries is not considered. Dispersion coefficients are assumed to be constants at all scales rather than scale-dependent variables as described by Gelhar (1993), Zhan (1998), and many others.

Notation

$C = C(x,y,z,t)$ concentration of point at time [M/L^3]
$\overline{C}$ $= \exp(\lambda t)C$
$\overline{C}_D$ $= (D_z)/(q_0 d^2)\overline{C}$, dimensionless $\overline{C}$
d aquifer thickness [L]
D_x, D_y, D_z longitudinal, transverse horizontal and vertical dispersion coefficients [L^2/T],
G Green's function
q_a area source strength function [M/(L^{2}T)]
q_l line source strength function [M/(LT)]
q_p point source strength function [M/T]
q_v $= q_0 f(t)$, volume source strength function [M/(L^{3}T)]
q_0 constant source strength [M/(L^{3}T)]
$\overline{q}_v$ $= \exp(\lambda t)q_v$
$\overline{q}_{vD}$ $= \overline{q}_v/q_0$
$S(M,t)$ source function
t time [T]
t_D $= ((D_z)/(d^2))t$, dimensionless time
v velocity of groundwater [M/T]
v_D $= (vd)/(\sqrt{D_x D_z})$, dimensionless velocity
x, y, z coordinates of the point where concentration is measured [L]
x_0, y_0, z_0, z_1 sources dimensions along the x-, y-, and z-axes [L]
x_D, y_D, z_D $x_D = (x/d)\sqrt{(D_z)/(D_x)}$, $y_D = (y/d)\sqrt{(D_z)/(D_y)}$, $z_D = z/d$, dimensionless x, y and z
$\bar{x}$ $= x - vt$
$\delta(\ )$ Dirac delta function
λ first-order decay factor [T]
ξ, ψ, ζ, τ, τ' dummy indexes for integration
ξ_D, ψ_D, ζ_D, τ_D, τ'_D dimensionless dummy index for integration.

Acknowledgements

Support for this work was provided by the U.S. National Science Foundation Grant No. BES-9909964 and by the Office of the Vice President for Research and Associate Provost for Graduate Studies, Texas A&M University through the Interdisciplinary Research Initiatives. Thanks to Dr. Hubao Zhang for providing useful references. We also thank two anonymous reviewers for their constructive comments.

References

Abramowitz, M., Stegun, I.A., 1972. Handbook of Mathematical Functions. Dover Publications, New York, USA.

Arfken, G.B., Weber, H.J., 1995. Mathematical Methods for Physicists, 4th edn. Academic Press, San Diego, USA.

Batu, V., 1989. A generalized two-dimensional analytical solution for hydrodynamic dispersion in bounded media with the first-type boundary condition at the source. Water Resour. Res. 25, 1125–1132.

Batu, V., 1993. A generalized two-dimensional analytical solute transport model in bounded media for flux-type finite multiple sources. Water Resour. Res. 29, 2881–2892.

Bear, J., 1972. Dynamics of Fluids in Porous Media. Elsevier, New York, USA.

Carslaw, H.S., Jaeger, J.C., 1959. Conduction of Heat in Solids. Clarendon Press, Oxford, UK.

Domenico, P.A., 1987. An analytical model for multidimensional transport of a decaying contaminant species. J. Hydrol. 91, 49–58.

Domenico, P.A., Robbins, G.A., 1984. A new method of contaminant plume analysis. Ground Water 23, 476–485.

Domenico, P.A., Schwartz, F.W., 1998. Physical and Chemical Hydrogeology. Wiley, New York, USA.

Fetter, C.W., 1999. Contaminant Hydrogeology, 2nd edn. Prentice-Hall, Upper Saddle River, NJ, USA.

Gelhar, L.W., 1993. Stochastic Subsurface Hydrology. Prentice-Hall, Englewood Cliffs, NJ, USA.

Gringarten, A.C., Ramey Jr., H.J., 1973. The use of source and Green's functions in solving unsteady-flow problems in reservoirs. Soc. Pet. Eng. J. 13, 285–296.

Leij, F.J., Toride, N., van Genuchten, M.Th., 1993. Analytical solutions for non-equilibrium solute transport in three-dimensional porous media. J. Contam. Hydrol. 151, 193–228.

Leij, F.J., Priesackand, E., Schaap, M.G., 2000. Solute transport modeled with Green's functions with application to persistent solute sources. J. Contam. Hydrol. 41, 155–173.

MathWorks, 2000. MATLAB (software), website: www.mathworks.com. Natick, MA, USA.

Morgenau, M., Murphy, G.M., 1956. The Mathematics of Physics and Chemistry. Van Nostrand, Princeton, NJ, USA.

Ogata, A., Banks, R.B., 1961. A solution of differential equation of longitudinal dispersion in porous media. U.S. Geol. Surv. Prof. Pap. 411, A1–A7.

Sauty, J.P., 1980. An analysis of hydrodispersive transfer in aquifers. Water Resour. Res. 16, 145–158.

van Genuchten, M.T., 1981. Analytical solutions for chemical transport with simultaneous adsorption, zero-order production and first-order decay. J. Hydrol. 49, 213–233.

Wexler, E.J., 1992. Analytical solutions for one-, two-, and three-dimensional solute transport in ground-water systems with uniform flow. U.S. Geological Survey, Techniques of Water-Resources Investigations, Book 3, Chap. B7.

Yeh, G.T., 1981. AT123D: analytical transient one-, two-, and three-dimensional simulation of waste transport in an aquifer system. Rep. ORNL-5602. Oak Ridge National Laboratory, Oak Ridge, TN.

Zhan, H., 1998. Transport of waste leakage in heterogeneous stratified formations. Adv. Water Resour. 22 (2), 159–168.

Zhan, H., 1999. Analytical study of capture time to a horizontal well. J. Hydrol. 217, 46–54.

Zheng, C., Bennett, G.D., 1995. Applied Contaminant Transport Modeling, Theory and Practice. Van Nostrand-Reinhold, New York, USA.